Multi-modal transfer-matrix method to compute the dispersion diagram of periodic structures

Francisco Mesa[1]

COST Action SyMat and the ESoA: EXPLOITING SYMMETRIES IN ARTIFICIAL MATERIALS FOR ANTENNA APPLICATIONS

COST ACTION CA18223
SYMAT
FUTURE COMMUNICATIONS WITH HIGHER-SYMMETRIC ENGINEERED ARTIFICIAL MATERIALS

[1]Dept. of Applied Physics 1, Universidad de Sevilla, Spain (mesa@us.es)

Outline

Background

Analysis

Results and Discussion

Concluding remarks

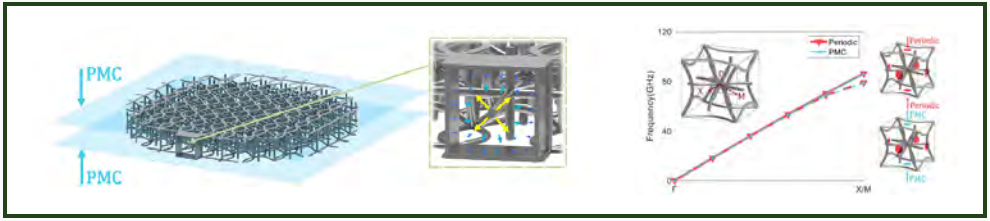
Background

Background and motivation - Periodic structures

Periodic structures are widely used to control the **propagation/scattering characteristics** of electromagnetic waves in many applications...

- Filters, couplers, phase shifters,. . .
- Frequency selective surfaces
- Leaky-wave antennas
- Metasurfaces and **Metalenses**

Periodicity gives rise to the **appearance of stop/rejection bands**. (🤔)
Complex geometries and large electrical size of structures
⇒**direct use of full-wave simulators becomes a computer-resource hungry procedure.**



[Wang et al, "Three-dimensional broadband and isotropic double-mesh twin-wire media for meta-lenses," Appl. Sci., vol. 11, no. 15, 2021]

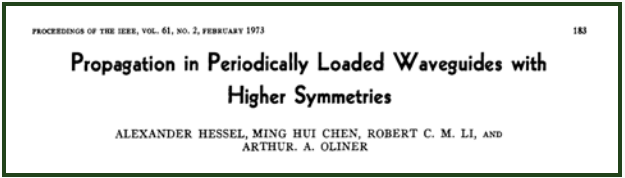
Background and motivation – Higher symmetries in periodic structures

Higher symmetries yield new characteristics that can provide additional control of the band structure of the structure.

More than simple translation/reflection.

Prof. Quevedo-Teruel and co-workers have been shown relevant design features:

- dispersion-less characteristics
- widening of transmission/rejection bands
- reduction of leakage in high-frequency transitions
- increase of on-axis anisotropy
- larger magnetic response,. . .



PROCEEDINGS OF THE IEEE, VOL. 61, NO. 2, FEBRUARY 1973 183

Propagation in Periodically Loaded Waveguides with Higher Symmetries

ALEXANDER HESSEL, MING HUI CHEN, ROBERT C. M. LI, AND ARTHUR. A. OLINER

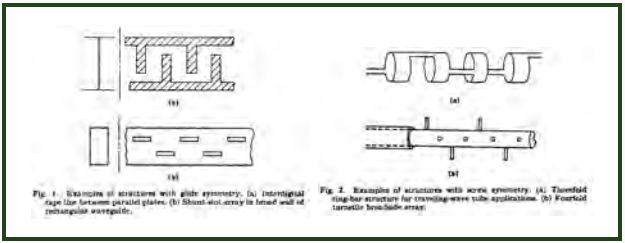


Fig. 1. Examples of structures with glide symmetry. (a) Interdigital cage line between parallel plates. (b) Shunt-slot array in broad wall of rectangular waveguide.

Fig. 2. Examples of structures with screw symmetry. (a) Threefold ring-bar structure for traveling-wave tube applications. (b) Fourfold turnstile broadside array.

Background and motivation – Dispersion relation



IEEE Journal of Microwaves

Received 26 August 2020; revised 11 October 2020; accepted 23 October 2020.
Date of current version 7 January 2021.

On the Benefits of Glide Symmetries for Microwave Devices

OSCAR QUEVEDO-TERUEL [1] (Senior Member, IEEE), QIAO CHEN [1] (Member, IEEE), FRANCISCO MESA [2] (Fellow, IEEE), NELSON J. G. FONSECA [3] (Senior Member, IEEE), AND GUIDO VALERIO [4,5] (Senior Member, IEEE)

(Invited Paper)

The knowledge of the dispersion diagram of the structure provides **essential information** about the performance of the structure and its eventual use in practical designs.

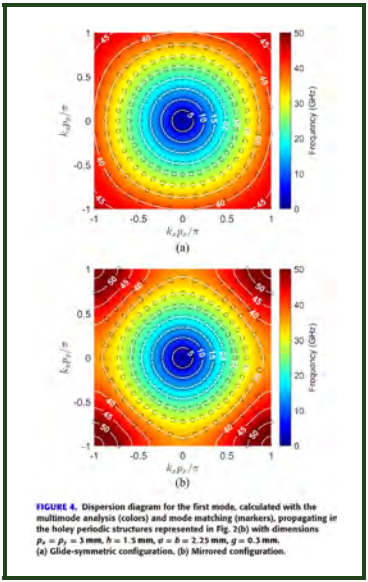
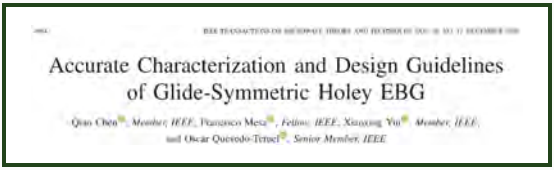


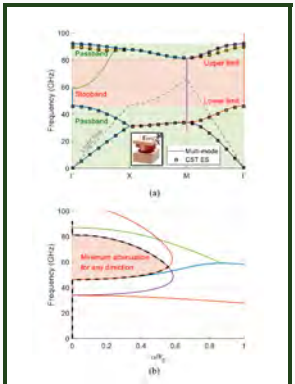
FIGURE 4. Dispersion diagram for the first mode, calculated with the multimode analysis (colors) and mode matching (markers), propagating in the holey periodic structures represented in Fig. 2(b) with dimensions $p_x = p_y = 3$ mm, $h = 1.5$ mm, $a = b = 2.25$ mm, $g = 0.3$ mm. (a) Glide-symmetric configuration. (b) Mirrored configuration.

Background and motivation – Dispersion relation & Look-up tables



Accurate Characterization and Design Guidelines of Glide-Symmetric Holey EBG

Qiao Chen, *Member, IEEE*, Francisco Mesa, *Fellow, IEEE*, Xiaoxing Yu, *Member, IEEE*, and Oscar Quevedo-Teruel, *Senior Member, IEEE*



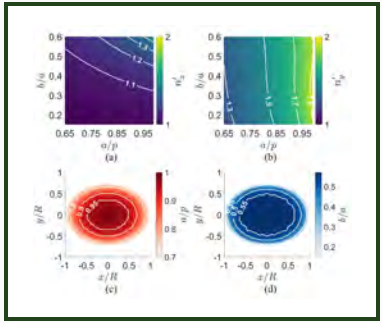


Applied Physics Letters

Anisotropic glide-symmetric substrate-integrated-holey metasurface for a compressed ultrawideband Luneburg lens

Cite as: Appl. Phys. Lett. 118, 084102 (2021)
Submitted: 24 December 2020 · Accepted: 9 February 2021 ·
Published Online: 25 February 2021

Qiao Chen, Federico Giusti, Guido Valerio, Francisco Mesa, and Oscar Quevedo-Teruel



Other works

Bloch Analysis of Artificial Lines and Surfaces Exhibiting Glide Symmetry

Mohammad Bagheriasl, Oscar Quevedo-Teruel, *Senior Member, IEEE*, and Guido Valerio, *Senior Member, IEEE*

symmetry

MDPI

Article

On the Computation of the Dispersion Diagram of Symmetric One-Dimensionally Periodic Structures

Francisco Mesa [1,*,†], Raúl Rodríguez-Berral [1,†] and Francisco Medina [2,†]



Francisco Mesa, Guido Valerio, Raúl Rodríguez-Berral, and Óscar Quevedo-Teruel

Simulation-Assisted Efficient Computation of the Dispersion Diagram of Periodic Structures

A comprehensive overview with applications to filters, leaky-wave antennas and metasurfaces.

Analysis

Obtaining of the dispersion diagram in homogeneous structures

In **homogeneous** waveguiding system [propagation given by $\exp(-\mathrm{j}(k_z z - \omega t))$, with $k_z = \beta_z - \mathrm{j}\alpha_z$], the dispersion diagram can rigorously be obtained from the corresponding **non-linear eigenvalue problem**:

$$[\mathbf{\Gamma}(k_z, \omega)][\mathbf{u}] = 0 \quad \Rightarrow \quad \boxed{\det\left[\mathbf{\Gamma}(k_z, \omega)\right] = 0}\,. \quad (🤔)$$

For fixed frequencies (ω_0), we have to compute the values of k_z that make

$$F(k_z) = 0 \quad \text{with} \quad F(k_z) \equiv \det\left[\mathbf{\Gamma}(k_z; \omega_0)\right]\,.$$

However, **searching for the complex zeros of a complex function** is not an easy task at all !!! (😰)

- Presence of poles and/or branch cuts creates a very intricate numerical scenario.
- Extreme difficulty in finding a systematic algorithm amenable to be implemented in a computer code.

A very similar discussion also holds for the case of periodic guiding systems.

Obtaining of the dispersion diagram in 1-D periodic structures

Although in-house numerical methods can be implemented for specific cases, 🤔
we focus here on a hybrid method assisted by **commercial full-wave electromagnetic simulators**.

Commercial simulators keep away from searching for **complex** zeros. (🙈)

Instead, a phase shift ($\Phi = \beta_z p$) is imposed between the periodic planes $z = 0$ and $z = p$.

A frequency sweeping is then carried out to find the frequency(ies) satisfying the phase condition.

No information about the attenuation constant (α_z) of the mode is directly provided. (🤫)

- Bandstop rejection level is not provided.
- *Large* material/radiation losses cannot be dealt with.
- Complex and leaky modes cannot be fully characterized.

. . . **Different alternatives are intensely searched for to compute the attenuation constant α_z**

S-parameters of a finite periodic structure with many unit cells

The output/input power ratio in a cascade of M unit cells satisfies

$$\exp(-2\alpha_z Mp) = |S_{11}|^2 + |S_{21}|^2$$

From the S-parameters simulated with the commercial full-wave solver, α_z/k_0 can be computed as

$$\boxed{\frac{\alpha_z}{k_0} = \frac{-\ln(|S_{11}|^2 + |S_{21}|^2)}{4\pi}\frac{\lambda_0}{Mp}}.$$

- ☺ This procedure can be applied to both closed and open structures.
- ☹ Convergence is often not achieved as M is increased.
- ☹ Very electrically-large structures have to be simulated...

2-port ABCD matrix of a single cell

From the transfer matrix (ABCD matrix) $[\mathbf{T}]$ of a single unit cell, $[\mathbf{T}] = \begin{bmatrix} A & B \\ C & D \end{bmatrix}$
obtained by means of either a commercial simulator or an in-house code,
and assuming that $\boxed{[\mathbf{T}_p] \approx [\mathbf{T}]}$ 🤨 ($[\mathbf{T}_p]$ is the unit-cell transfer matrix of the **periodic** structure),

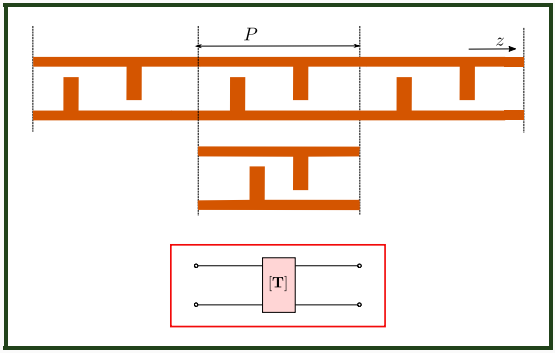
the following **standard eigenvalue problem**
($[\mathbf{A}]\mathbf{u} = \lambda\mathbf{u}$) can be set up:

$$[\mathbf{T}_p] \begin{bmatrix} V \\ I \end{bmatrix} = \mathrm{e}^{-jk_z p} \begin{bmatrix} V \\ I \end{bmatrix} .$$

Dispersion equation can **directly be calculated** as

$$\cos(k_z p) = \frac{A(\omega) + D(\omega)}{2}$$

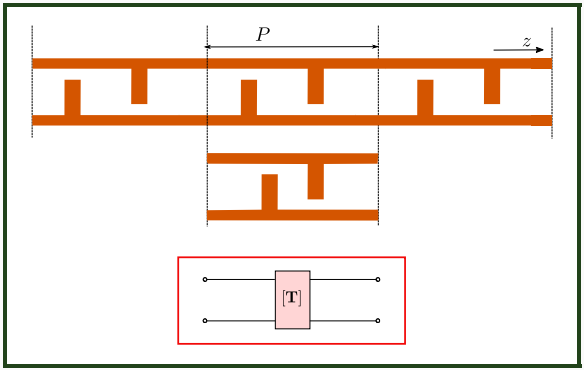
Function arcos( ) is **multivalued**!! (😟)



Interactions between cells through high-order modes are **not** taken into account. (🤔)

Recommendations for obtaining the 2-port ABCD matrix of a single cell

- **Boundaries** of the unit cell should be **electrically far from** the discontinuity.
  The “housing” waveguide (input/output ports) should be easily recognizable, when possible.
- **Internal symmetries** inside the unit cell should be preserved (existence of EW, MW, mirror planes,...)



It should work well as long as **interactions between cells** through high-order modes are **negligible**.

2-port ABCD matrix of a cascade of N cells (Method A)

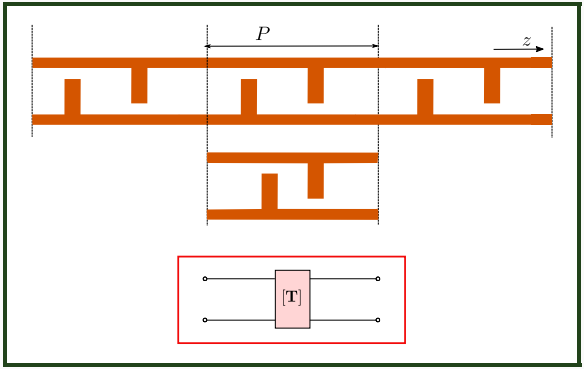
Obtaining of the 2-port transfer matrix (ABCD matrix), $[\mathbf{T}_N]$, of a **finite stack of N unit cells** by means of a commercial simulator.

$$[\mathbf{T}_N] = \begin{bmatrix} A_N & B_N \\ C_N & D_N \end{bmatrix} \Rightarrow \boxed{[\mathbf{T}_p] \approx \sqrt[N]{[\mathbf{T}_N]}} = \begin{bmatrix} A_p & B_p \\ C_p & D_p \end{bmatrix}$$

From $[\mathbf{T}_N]$, the equivalent **effective** periodic transfer matrix $[\mathbf{T}_p]$ is extracted.

The dispersion equation is now directly obtained as

$$\boxed{\cos(k_z p) = \frac{A_p + D_p}{2}}$$



Interactions between cells through high-order modes are **partially** accounted for.

Simulation of a cascade of N cells

☺ Interactions between adjacent unit cells through **high-order modes** is partially taken into account (only well accounted for if $N \gg 1$).

☺ No numerical searching for the solution of $k_z p$.

☹ The **computational effort** might be very high because of the large size of the structure.

☹ Appearance of **spurious** solutions [*]. It can be checked that, in general, $\sqrt[N]{[\mathbf{A}]^N} \neq [\mathbf{A}]$ (🤔)

☹ Existence of **numerical noise**.
Very relevant if attenuation of periodic leaky-wave antennas is to be computed.

☹ **Ambiguity** of the phase constant due to "folding" of the first Brillouin zone [*].

[*] G. Valerio et al, "Accurate Bloch analysis of 1-D periodic lines through the simulation of truncated structures," *IEEE Trans. Antennas Propag.* **2011**, *59*, 2188–2195

Alternative 2-port ABCD matrix of a cascade of N cells (Method A)

Calculate the 2-port transfer matrices $[\mathbf{T}_{N+1}]$ and $[\mathbf{T}_N]$, of a **finite stack of $N+1$ and N unit cells** by means of a commercial simulator.

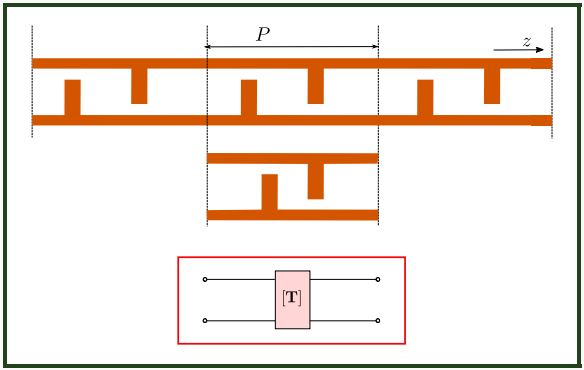
Now we assume that $[\mathbf{T}_{N+1}] \approx [\mathbf{T}_N][\mathbf{T}_p]$.

From $[\mathbf{T}_{N+1}]$ and $[\mathbf{T}_N]$, the equivalent **effective** periodic transfer matrix $[\mathbf{T}_p]$ is extracted as

$$[\mathbf{T}_p] \approx [\mathbf{T}_N]^{-1}[\mathbf{T}_{N+1}]$$

The dispersion equation is directly obtained as

$$\cos(k_z p) = \frac{A_p + D_p}{2}$$



Interactions between cells through high-order modes are **partially** accounted for.

Simulation of a cascade of $N+1$ and N cells

- ☺ Interactions between adjacent unit cells through **high-order modes** is partially taken into account (only well accounted for if $N \gg 1$).
- ☺ No numerical searching for the solution of $k_z p$.
- ☹ No previous knowledge of what value of N ensures convergence/stability of results.
- ☹ The **computational effort** might be very high because of the possible large size of the structure.
- ☹ Existence of **numerical noise**.
  Very relevant if attenuation of periodic leaky-wave antennas is to be computed.

Multi-port(mode) ABCD matrix of a single cell (Method B [MMTMM])

The multi-port(mode) transfer matrix $[\mathbf{T}]$ of a **single** unit cell [Collin, "Field Theory of Guided Waves", p. 627]

$$[\mathbf{T}] = \begin{bmatrix} [\mathbf{A}] & [\mathbf{B}] \\ [\mathbf{C}] & [\mathbf{D}] \end{bmatrix} \qquad [\mathbf{A}], [\mathbf{B}], [\mathbf{C}], [\mathbf{D}] : \ N \times N \text{ submatrices}$$

can be computed by means of a commercial simulator; for instance, from the generalized scattering matrix

$$[\mathbf{A}] = \frac{1}{2}\left[([\mathbf{1}] + [\mathbf{S}_{11}])\,[\mathbf{S}_{21}]^{-1}\,([\mathbf{1}] - [\mathbf{S}_{22}]) + [\mathbf{S}_{12}]\right]$$

$$[\mathbf{B}] = \frac{1}{2}\left[(([\mathbf{1}] + [\mathbf{S}_{11}])\,[\mathbf{S}_{21}]^{-1}\,([\mathbf{1}] + [\mathbf{S}_{22}]) - [\mathbf{S}_{12}])\,[\mathbf{Z}_o]\right]$$

$$[\mathbf{C}] = \frac{1}{2}\left[[\mathbf{Z}_i]^{-1}\left(([\mathbf{1}] - [\mathbf{S}_{11}])\,[\mathbf{S}_{21}]^{-1}\,([\mathbf{1}] - [\mathbf{S}_{22}]) - [\mathbf{S}_{12}]\right)\right]$$

$$[\mathbf{D}] = \frac{1}{2}\left[[\mathbf{Z}_i]^{-1}\left(([\mathbf{1}] - [\mathbf{S}_{11}])\,[\mathbf{S}_{21}]^{-1}\,([\mathbf{1}] + [\mathbf{S}_{22}]) + [\mathbf{S}_{12}]\right)[\mathbf{Z}_o]\right] \ .$$

$[\mathbf{1}]$: identity matrix, $[\mathbf{Z}_{i/o}]$: diagonal matrix that contains the impedance of the N input/output (i/o) port modes.

Multi-port(mode) ABCD matrix of a single cell (Method B [MMTMM])

From the multi-port(mode) transfer matrix $[\mathbf{T}]$ of a **single** unit cell

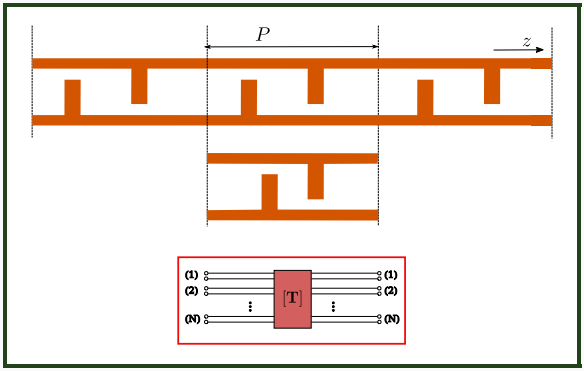
$$[\mathbf{T}] = \begin{bmatrix} [\mathbf{A}] & [\mathbf{B}] \\ [\mathbf{C}] & [\mathbf{D}] \end{bmatrix}$$

the dispersion equation comes from the solution of the following standard eigenproblem ($2N \times 2N$):

$$\left\{ [\mathbf{T}] - \mathrm{e}^{-jk_z p}[\mathbf{1}] \right\} \begin{bmatrix} \mathbf{V} \\ \mathbf{I} \end{bmatrix} = 0 \, .$$

If the unit cell is reciprocal and symmetric ($[\mathbf{A}] = [\mathbf{D}]^T$, $[\mathbf{B}] = [\mathbf{B}]^T$, and $[\mathbf{C}] = [\mathbf{C}]^T$)

$$\{[\mathbf{A}] - \cos(k_z p)[\mathbf{1}]\}\, \mathbf{V} = 0$$



Interactions between cells through high-order modes are **well** accounted for. (🙂)

Invariance of the eigenproblem under the impedance port definition

The multi-mode transfer matrix can be written as

$$[\mathbf{T}] = \begin{bmatrix} [\mathbf{1}] & [\mathbf{0}] \\ [\mathbf{0}] & [\mathbf{Z}_i]^{-1} \end{bmatrix} [\mathbf{T}_U] \begin{bmatrix} [\mathbf{1}] & [\mathbf{0}] \\ [\mathbf{0}] & [\mathbf{Z}_o] \end{bmatrix}$$

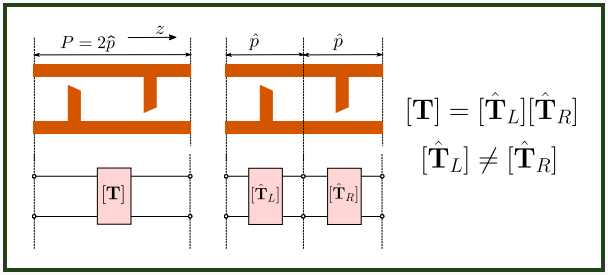
- $[\mathbf{T}_U]$ stands for the transfer matrix defined with **unitary port impedances**.
- As long as $[\mathbf{Z}_i] = [\mathbf{Z}_o]$, the eigenproblem for $[\mathbf{T}]$ is equivalent to the one for $[\mathbf{T}_U]$.

The **eigenproblem is invariant** under a change of the impedances of the input/output ports

- Valid for situations even though the original port impedances are imaginary...

Existence of higher symmetries in the unit cell

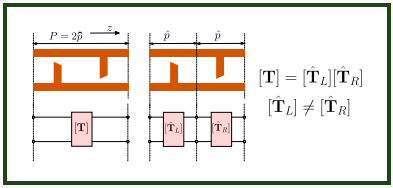
Glide symmetry: Reflection in the central horizontal plane + translation of half period.



Generalized Floquet's theorem allows us to write the eigenvalue problem for the sub-unit cell ($\hat{p} = P/2$)

$$[\mathbf{T}] \begin{bmatrix} \mathbf{V} \\ \mathbf{I} \end{bmatrix} = \mathrm{e}^{-jk_z P} \begin{bmatrix} \mathbf{V} \\ \mathbf{I} \end{bmatrix} \quad \Longrightarrow \quad [\widehat{\mathbf{T}}] \begin{bmatrix} \mathbf{V} \\ \mathbf{I} \end{bmatrix} = \mathrm{e}^{-jk_z \hat{p}} \begin{bmatrix} [\mathbf{Q}] & [\mathbf{0}] \\ [\mathbf{0}] & [\mathbf{Q}] \end{bmatrix} \begin{bmatrix} \mathbf{V} \\ \mathbf{I} \end{bmatrix}$$

Glide symmetry in the unit cell



$$[\widehat{\mathbf{T}}]\begin{bmatrix}\mathbf{V}\\ \mathbf{I}\end{bmatrix} = \mathrm{e}^{-jk_z\hat{p}}\begin{bmatrix}[\mathbf{Q}] & [\mathbf{0}]\\ [\mathbf{0}] & [\mathbf{Q}]\end{bmatrix}\begin{bmatrix}\mathbf{V}\\ \mathbf{I}\end{bmatrix}$$

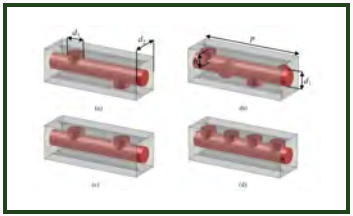
- $[\widehat{\mathbf{T}}]$ is the corresponding multiport transfer matrix for the sub-unit cell.
- $[\mathbf{Q}]$ accounts for the corresponding algebraic operations associated with the glide symmetry.

For glide symmetry: $[\mathbf{Q}] = \begin{bmatrix} \begin{bmatrix} q_{11} & 0 \\ 0 & q_{11} \end{bmatrix} & & & \\ & \ddots & & \\ & & \begin{bmatrix} q_{ii} & 0 \\ 0 & q_{ii} \end{bmatrix} & \\ & & & \ddots \\ & & & \begin{bmatrix} q_{NN} & 0 \\ 0 & q_{NN} \end{bmatrix} \end{bmatrix}$

$$q_{ii} = \begin{cases} +1 & \text{if } i\text{-th mode is even} \\ -1 & \text{if } i\text{-th mode is odd} \end{cases}$$

More details in [F. Mesa et al, "Simulation-Assisted Efficient Computation of the Dispersion Diagram of Periodic Structures," *IEEE Antennas Propag. Mag.*, https://doi.org/10.1109/MAP.2020.3003210]

Twist symmetry in the unit cell



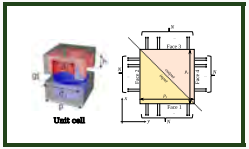
$$[\mathbf{T}_{1/N}]\begin{bmatrix}\mathbf{V}\\ \mathbf{I}\end{bmatrix} = \mathrm{e}^{-jk_z p/N}\begin{bmatrix}[\mathbf{Q}] & [\mathbf{0}]\\ [\mathbf{0}] & [\mathbf{Q}]\end{bmatrix}\begin{bmatrix}\mathbf{V}\\ \mathbf{I}\end{bmatrix}$$

- $[\mathbf{T}_{1/N}]$ is the multiport transfer matrix for the 1/N sub-unit cell. *N*: order of the twist symmetry.
- $[\mathbf{Q}]$ accounts for the corresponding algebraic operations associated with the twist symmetry.

Twist Symmetry: $[\mathbf{Q}] = \begin{bmatrix} \begin{bmatrix} q_{11} & 0 \\ 0 & q_{11} \end{bmatrix} & & & \\ & \ddots & & \\ & & \begin{bmatrix} q_{ii} & 0 \\ 0 & q_{ii} \end{bmatrix} & \\ & & & \ddots \\ & & & \begin{bmatrix} q_{NN} & 0 \\ 0 & q_{NN} \end{bmatrix} \end{bmatrix}$ $q_{ii} = \exp\left(-jm\frac{2\pi}{N}\right)$

More details in [M. Bagheriasl and G. Valerio, "Bloch analysis of electromagnetic waves in twist-symmetric lines," *Symmetry* , vol. 11, no. 5, pp. 1–11, 2019, doi: 10.3390/sym11050620.]

MMTMM for 2-D periodic structures



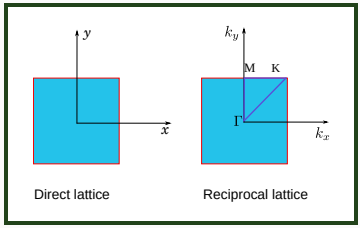
$$\begin{bmatrix}\mathbf{V}_1\\ \mathbf{V}_2\\ \mathbf{I}_1\\ \mathbf{I}_2\end{bmatrix} = [\mathbf{T}] \begin{bmatrix}\mathbf{V}_3\\ \mathbf{V}_4\\ \mathbf{I}_3\\ \mathbf{I}_4\end{bmatrix}, \quad \text{PBC's also impose} \quad \begin{bmatrix}\mathbf{V}_1\\ \mathbf{V}_2\\ \mathbf{I}_1\\ \mathbf{I}_2\end{bmatrix} = \begin{bmatrix}\mathrm{e}^{-jk_xp_x}\mathbf{V}_3\\ \mathrm{e}^{-jk_yp_y}\mathbf{V}_4\\ \mathrm{e}^{-jk_xp_x}\mathbf{I}_3\\ \mathrm{e}^{-jk_yp_y}\mathbf{I}_4\end{bmatrix}$$

The following (**non-standard** 🤔) eigenvalue problem can then be written:

$$[\mathbf{T}] \begin{bmatrix}\mathbf{V}_x\\ \mathbf{V}_y\\ \mathbf{I}_x\\ \mathbf{I}_y\end{bmatrix} = [\mathbf{B}(k_xp_x, k_yp_y)] \begin{bmatrix}\mathbf{V}_x\\ \mathbf{V}_y\\ \mathbf{I}_x\\ \mathbf{I}_y\end{bmatrix} \quad \text{with} \quad [\mathbf{B}] = \begin{bmatrix}\mathrm{e}^{-jk_xp_x}[\mathbf{1}] & [\mathbf{0}] & [\mathbf{0}] & [\mathbf{0}]\\ [\mathbf{0}] & \mathrm{e}^{-jk_yp_y}[\mathbf{1}] & [\mathbf{0}] & [\mathbf{0}]\\ [\mathbf{0}] & [\mathbf{0}] & \mathrm{e}^{-jk_xp_x}[\mathbf{1}] & [\mathbf{0}]\\ [\mathbf{0}] & [\mathbf{0}] & [\mathbf{0}] & \mathrm{e}^{-jk_yp_y}[\mathbf{1}]\end{bmatrix}$$

$\mathbf{V}_x$ is the N-port voltage array at "Face 3", whose BC is imposed along the x direction.

MMTMM for 2-D periodic structures. Obtaining of the dispersion diagram.



$$[\mathbf{T}]\begin{bmatrix}\mathbf{V}_x\\ \mathbf{V}_y\\ \mathbf{I}_x\\ \mathbf{I}_y\end{bmatrix} = [\mathbf{B}(\lambda_x,\lambda_y)]\begin{bmatrix}\mathbf{V}_x\\ \mathbf{V}_y\\ \mathbf{I}_x\\ \mathbf{I}_y\end{bmatrix}$$

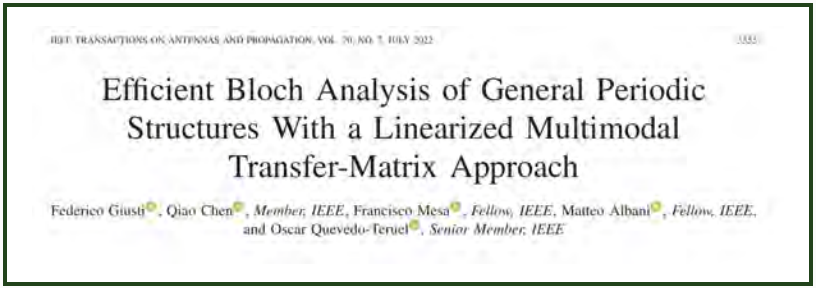
$$\lambda_x = \mathrm{e}^{-\mathrm{j}k_x p_x} \quad , \quad \lambda_x = \mathrm{e}^{-\mathrm{j}k_y p_y}$$

The ΓMK band diagram is obtained after **zero searching in the complex plane** for a particular solution to

$$\det\{[\mathbf{T}(\omega)] - [\mathbf{B}(\lambda_x,\lambda_y)]\} = 0$$

- ΓM path: $k_x p_x = 0$. Solve $f(\omega,\lambda_y) = 0$, with $f(\omega,\lambda_y) = \det\{[\mathbf{T}(\omega)] - [\mathbf{B}(\lambda_x = 1,\lambda_y)]\}$.
- MK path: $k_y p_y = \pi$. Solve $f(\omega,\lambda_x) = 0$, with $f(\omega,\lambda_x) = \det\{[\mathbf{T}(\omega)] - [\mathbf{B}(\lambda_x,\lambda_y = -1)]\}$.
- $K\Gamma$ path: $k_x p_x = k_y p_y \Rightarrow \lambda_x = \lambda_y \equiv \lambda$. Solve the standard eigenvalue problem: $[\mathbf{T}]\mathbf{W} = \lambda\mathbf{W}$.

MMTMM for 2-D periodic structures – Alternative approach



IEEE TRANSACTIONS ON ANTENNAS AND PROPAGATION, VOL. 70, NO. 7, JULY 2022 5335

Efficient Bloch Analysis of General Periodic Structures With a Linearized Multimodal Transfer-Matrix Approach

Federico Giusti, Qiao Chen, *Member, IEEE*, Francisco Mesa, *Fellow, IEEE*, Matteo Albani, *Fellow, IEEE*, and Oscar Quevedo-Teruel, *Senior Member, IEEE*

The non-standard eigenvalue problem $[\mathbf{T}] \begin{bmatrix} \mathbf{V}_x \\ \mathbf{V}_y \\ \mathbf{I}_x \\ \mathbf{I}_y \end{bmatrix} = \begin{bmatrix} \lambda_x \mathbf{V}_x \\ \lambda_y \mathbf{V}_y \\ \lambda_x \mathbf{I}_x \\ \lambda_y \mathbf{I}_y \end{bmatrix}$ can be written as $[\widetilde{\mathbf{T}}] \begin{bmatrix} \mathbf{V}_x \\ \mathbf{I}_x \\ \mathbf{V}_y \\ \mathbf{I}_y \end{bmatrix} = \begin{bmatrix} \lambda_x \mathbf{V}_x \\ \lambda_x \mathbf{I}_x \\ \lambda_y \mathbf{V}_y \\ \lambda_y \mathbf{I}_y \end{bmatrix}$

MMTMM for 2-D periodic structures – Alternative approach

$$[\widetilde{\mathbf{T}}]\begin{bmatrix}\mathbf{V}_x\\ \mathbf{I}_x\\ \mathbf{V}_y\\ \mathbf{I}_y\end{bmatrix}=\begin{bmatrix}\lambda_x\mathbf{V}_x\\ \lambda_x\mathbf{I}_x\\ \lambda_y\mathbf{V}_y\\ \lambda_y\mathbf{I}_y\end{bmatrix} \quad \text{is rewritten as} \quad \begin{bmatrix}[\widetilde{\mathbf{T}}_{xx}] & [\widetilde{\mathbf{T}}_{xy}]\\ [\widetilde{\mathbf{T}}_{yx}] & [\widetilde{\mathbf{T}}_{yy}]\end{bmatrix}\begin{bmatrix}\mathbf{F}_x\\ \mathbf{F}_y\end{bmatrix}=\begin{bmatrix}\lambda_x\mathbf{F}_x\\ \lambda_y\mathbf{F}_y\end{bmatrix}, \quad \text{with } \mathbf{F}_\alpha=\begin{bmatrix}\mathbf{V}_\alpha\\ \mathbf{I}_\alpha\end{bmatrix}.$$

Taking into account that $[\widetilde{\mathbf{T}}_{yx}]\mathbf{F}_x+[\widetilde{\mathbf{T}}_{yy}]\mathbf{F}_y=\lambda_y\mathbf{F}_y \quad \Rightarrow \quad \mathbf{F}_y=\left(\lambda_y[\mathbf{1}]-[\widetilde{\mathbf{T}}_{yy}]\right)^{-1}[\widetilde{\mathbf{T}}_{yx}]\mathbf{F}_x$,

the following two **standard eigenvalue problems** can be written:

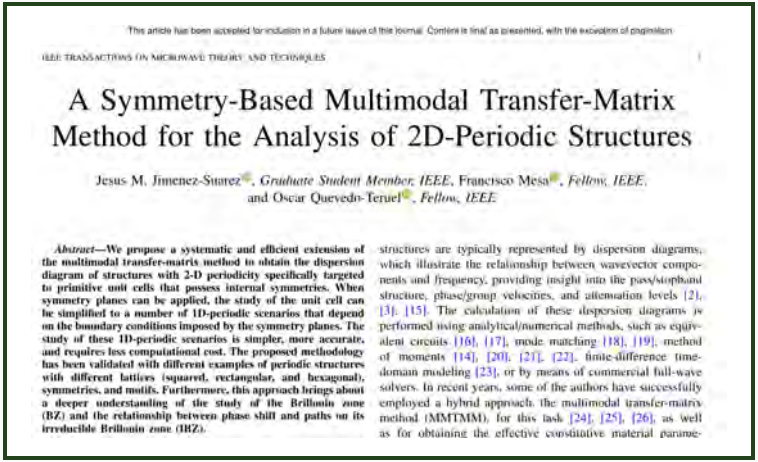
$$\left\{[\widetilde{\mathbf{T}}_{xx}]+[\widetilde{\mathbf{T}}_{xy}]\left(\lambda_y[\mathbf{1}]-[\widetilde{\mathbf{T}}_{yy}]\right)^{-1}[\widetilde{\mathbf{T}}_{yx}]\right\}\mathbf{F}_x=\lambda_x\mathbf{F}_x$$

$$\left\{[\widetilde{\mathbf{T}}_{yy}]+[\widetilde{\mathbf{T}}_{yx}]\left(\lambda_x[\mathbf{1}]-[\widetilde{\mathbf{T}}_{xx}]\right)^{-1}[\widetilde{\mathbf{T}}_{xy}]\right\}\mathbf{F}_y=\lambda_y\mathbf{F}_y$$

along paths where either λ_y or λ_x is **fixed** (namely, paths ΓM and MK).

No searching in the complex plane is required!!! ☺

2-D periodic structure. Symmetries



This article has been accepted for inclusion in a future issue of this journal. Content is final as presented, with the exception of pagination.

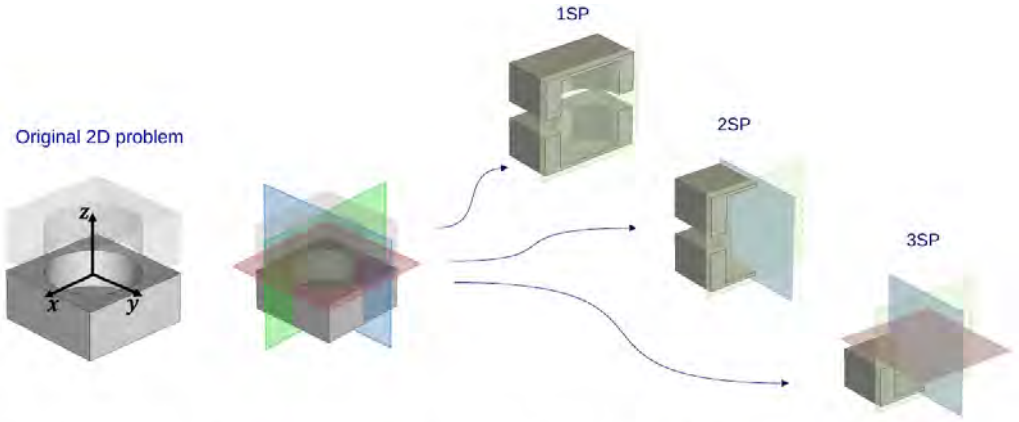
A Symmetry-Based Multimodal Transfer-Matrix Method for the Analysis of 2D-Periodic Structures

Jesus M. Jimenez-Suarez, *Graduate Student Member, IEEE*, Francisco Mesa, *Fellow, IEEE*, and Oscar Quevedo-Teruel, *Fellow, IEEE*

***Abstract*—We propose a systematic and efficient extension of the multimodal transfer-matrix method to obtain the dispersion diagram of structures with 2-D periodicity specifically targeted to primitive unit cells that possess internal symmetries. When symmetry planes can be applied, the study of the unit cell can be simplified to a number of 1D-periodic scenarios that depend on the boundary conditions imposed by the symmetry planes. The study of these 1D-periodic scenarios is simpler, more accurate, and requires less computational cost. The proposed methodology has been validated with different examples of periodic structures with different lattices (squared, rectangular, and hexagonal), symmetries, and motifs. Furthermore, this approach brings about a deeper understanding of the study of the Brillouin zone (BZ) and the relationship between phase shift and paths on its irreducible Brillouin zone (IBZ).**

structures are typically represented by dispersion diagrams, which illustrate the relationship between wavevector components and frequency, providing insight into the pass/stopband structure, phase/group velocities, and attenuation levels [2], [3]. [15]. The calculation of these dispersion diagrams is performed using analytical/numerical methods, such as equivalent circuits [16], [17], mode matching [18], [19], method of moments [14], [20], [21], [22], finite-difference time-domain modeling [23], or by means of commercial full-wave solvers. In recent years, some of the authors have successfully employed a hybrid approach, the multimodal transfer-matrix method (MMTMM), for this task [24], [25], [26], as well as for obtaining the effective constitutive material parame-

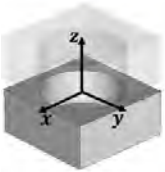
2-D periodic structure. Symmetries. Decomposition into simpler problems



- Several symmetry planes (SP) can be applied to reduce the complexity of the original 2D problem.
- Different 1D problems are generated by imposing a varying number of symmetry planes.

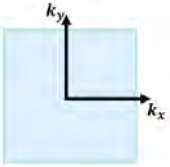
2-D periodic structure. Symmetries

Physical space

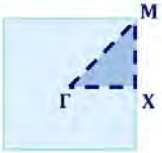


Reciprocal space

Brillouin zone



Irreducible Brillouin zone



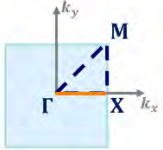
IBZ path	Phase shift

- The unit cell is studied in the reciprocal space (wavenumber space).
- The **Brillouin zone** (BZ) contains all the information of the wave propagation properties.
- **Irreducible Brillouin zone** (IBZ) has the minimal information to know where the stopbands are located.

2-D periodic structure. Symmetries: Path $\overline{\Gamma X}$

$\overline{\Gamma X}$ path

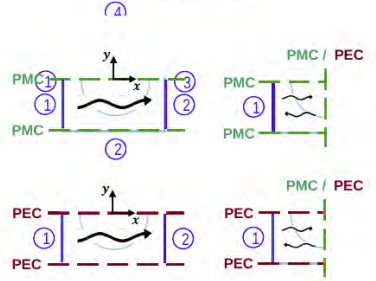
Reciprocal space



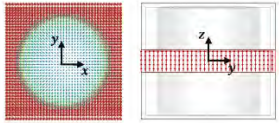
$k_y = 0, \pm 2n\pi$

$k_x = [0, \pi]$

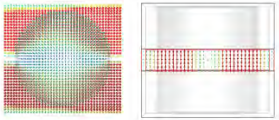
Physical space



$\Delta\phi_y = 0$

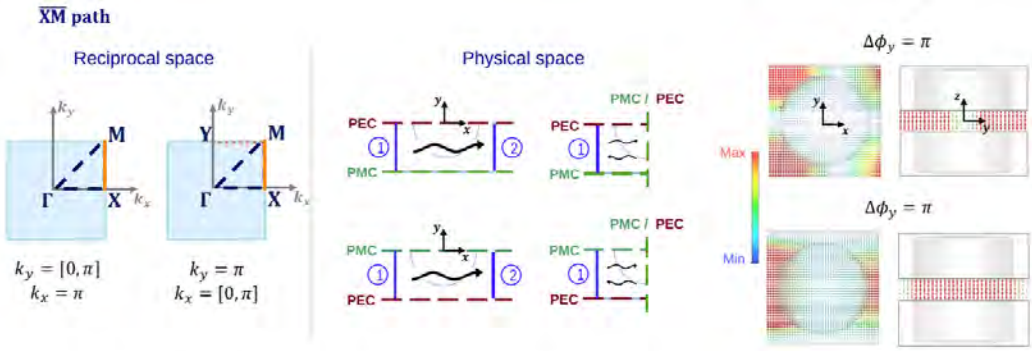


$\Delta\phi_y = 2\pi$



- The **irreducible Brillouin zone** (IBZ) can be **simulated using symmetry planes**.
- The **number of ports** used in the simulation is **reduced** from 4 to 1.

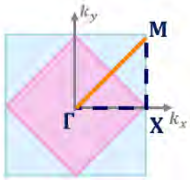
2-D periodic structure. Symmetries: Path $\overline{XM}$

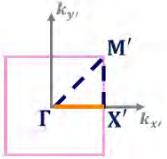


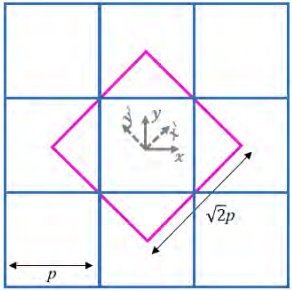
- The path $\overline{YM}$ is equivalent to the path $\overline{XM}$ due to the symmetry of the unit cell.
- The **number of ports** used in the simulation is **reduced** from 4 to 1.

2-D periodic structure. Symmetries: Path $\overline{\Gamma M}$

$\overline{\Gamma M}$ path





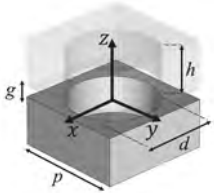


- A **rotated supercell** of size $\sqrt{2}p$ is necessary to compute the $\overline{\Gamma M}$.
- The **$\overline{\Gamma M}$ path is obtained when $\overline{\Gamma X'}$ is solved** in the supercell.
- The phase delay $\boldsymbol{\Delta\phi_{y'} = 0}$ must be ensured.

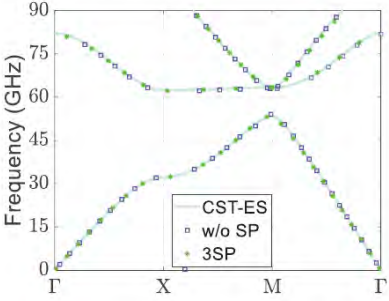




2-D periodic structure. Symmetries: Brillouin Diagram



Path	$\Delta\phi_x$	$\Delta\phi_y$
ΓX	$[0, \pi]$	$0, \pm 2n\pi$
XM	$\pm(2n+1)\pi$	$[0, \pi]$
ΓM	$\phi_x = \phi_y$	$[0, \pi]$; $[\pm 2n\pi, \pm(2n+1)\pi]$



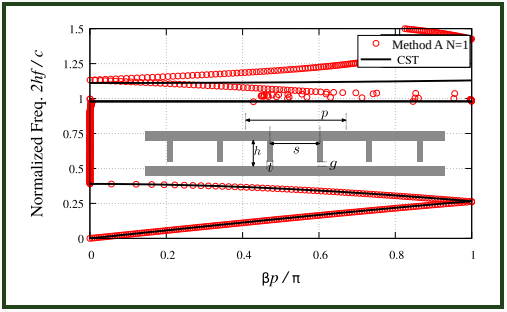
Results and Discussion

Long Period: $h = 10t, g = 2t, s = 10t, p = 22t = 2.2h$

The differences between these two long-period PPW structures are small for $f < f_c[= c/(2h)]$. (🤔)

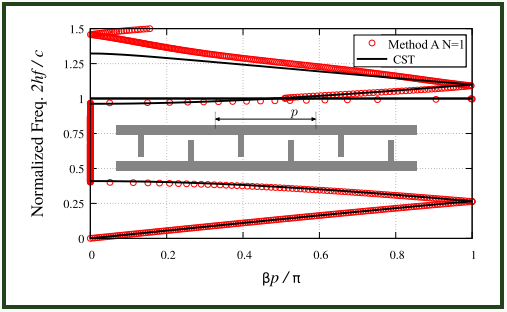
Both inter-cell and intra-cell interactions are well accounted for by only the fundamental mode.

Standard periodicity



- "Method A N=5" identical to "Method A N=1"
- No agreement expected with CST-ES beyond the onset frequency of high-order modes.

Glide Symmetry



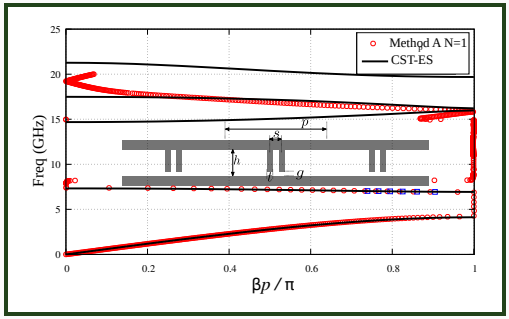
- "Method A N=5" identical to "Method A N=1"
- Glide symmetry does not play any role here in the first propagation band.

Long Period: $p = 12$ mm, $h = 10$ mm, $s = 2$ mm, $t = 1$ mm, and $g = 1$ mm.

Long-period: Interactions between cells should be well accounted for by only the fundamental mode.

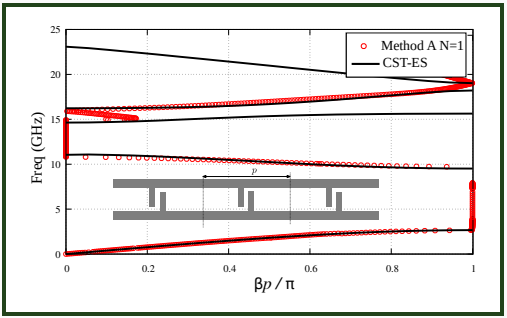
Differences between the two structures comes from **high-order interactions** between the posts. (🙄)

Reflection Symmetry



- "Method A N=5" identical to "Method A N=1"
- No agreement with CST-ES beyond the cutoff frequency of the 1st HOM of the PPW (15 GHz).

Inversion Symmetry

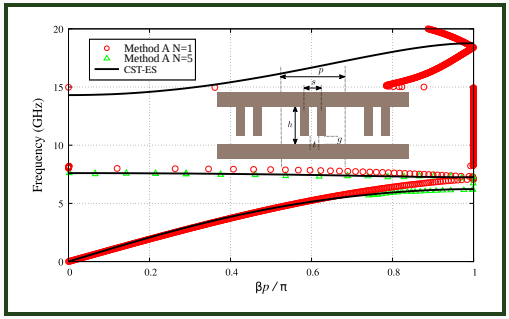


- "Method A N=5" identical to "Method A N=1"
- Reduced first propagation band

Medium Period: $p = 6$ mm

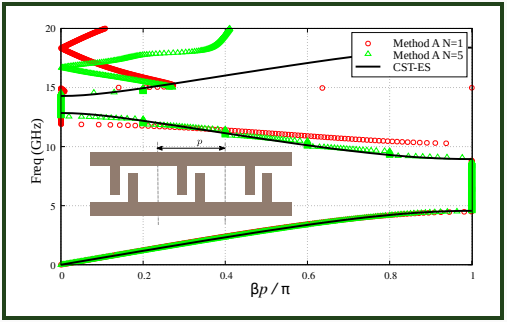
High-order interactions between cells start being relevant. (😏)

Reflection Symmetry



- “N=5” $\sim$ “N=1” only at low frequencies
- “Method A” not reliable beyond f_c (🤔)

Inversion Symmetry



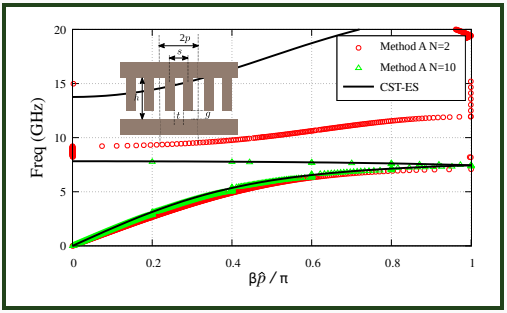
- “N=5” $\sim$ “N=1” up to medium frequencies
- Reduced first propagation band

Short Period. Conventional symmetry vs. Glide symmetry

High-order interactions between cells are relevant at lower frequencies. (🤨)

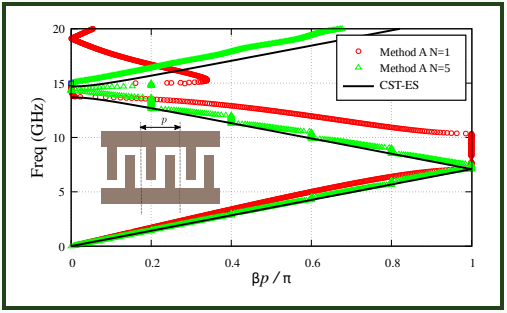
Significant effects of glide symmetry can clearly be appreciated!

Non-glide Symmetry, $\hat{p} = 2p$



- “N=10” ≈ “N=2” only at low frequencies
- “Method A” not reliable outside first pass band

Glide Symmetry



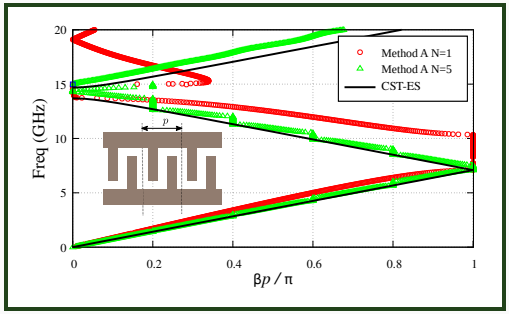
- “N=5” ≈ “N=1” only at low frequencies
- “N=5” ≈ “CST-ES” in the considered range

Glide symmetry. Method A vs. Method B

High-order interactions between cells are very relevant.

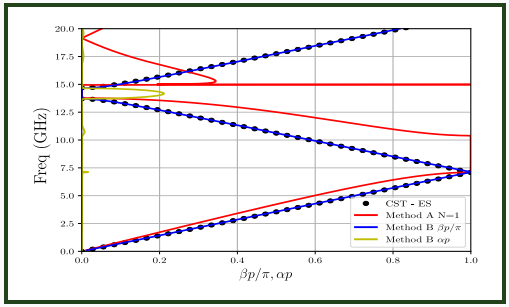
Significant effects of glide symmetry can clearly be appreciated!

Glide Symmetry. **Method A**



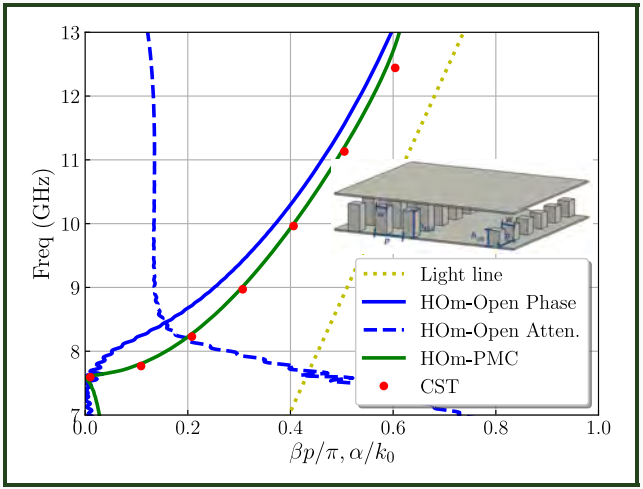
- “N=5” $\sim$ “N=1” only at very low frequencies
- “N=5” $\sim$ “CST-ES” in the considered range

Glide Symmetry. **Method B**



- “Method B” provides accurate results (😌)
- The attenuation constant is well accounted for

Groove-gap waveguide

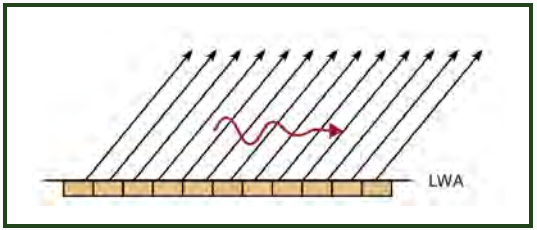


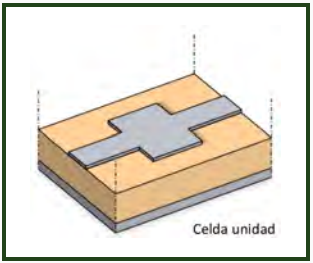
The groove waveguide corresponds to the standard WR-90.
The dimensions are: w = 3 mm, p = 8.5 mm, h_{LW} = 3.5 mm, h_{EBG} = 7.5 mm.

1-D Open Structures

The analysis of periodic structure is challenging.

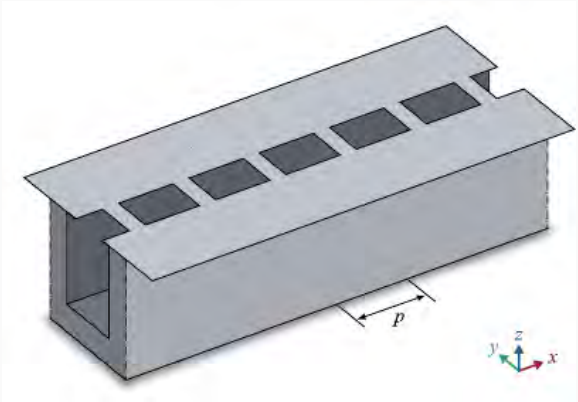
- The spectrum is **discrete** (surface waves + proper backward leaky modes) + **continous**.
- The radiative part of the CS can eventually be well characterized by improper forward leaky modes.
- Proper/improper leaky modes have **complex** wavenumbers.
- The boundaries of the unit cell are not well defined.

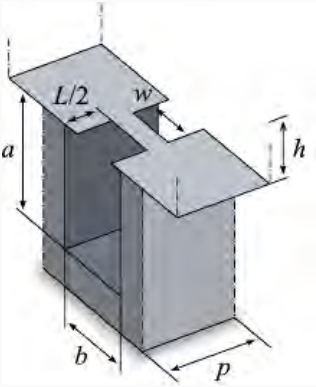




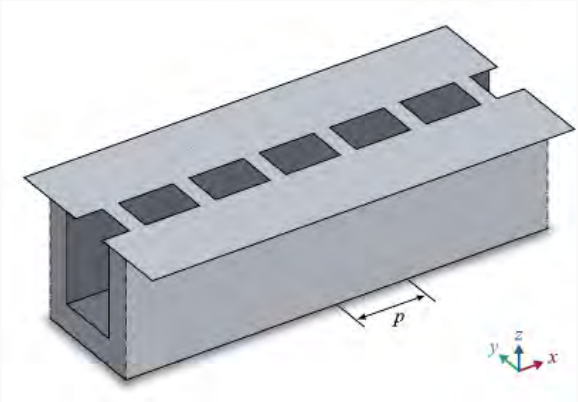
[S. Garcia-Martinez, F. Giusti, F. Mesa, A. Tamayo-Dominguez and O. Quevedo-Teruel, "Accurate Full-Wave Bloch Analysis of General 1D-Periodic Open Structures," in IEEE Transactions on Antennas and Propagation, 10.1109/TAP.2025.3587901, (Early Access)]

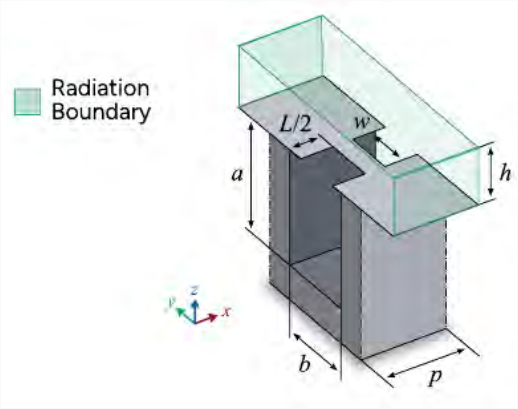
1-D Open Structures: Slotted Rectangular Waveguide



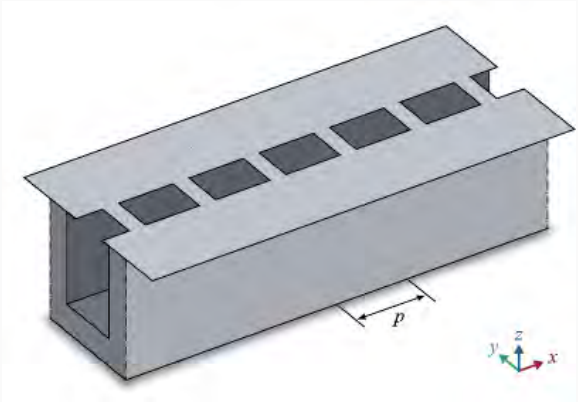


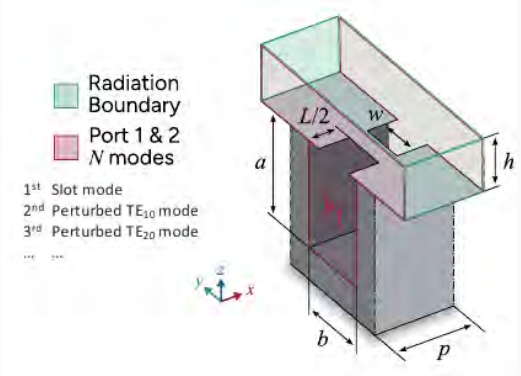
1-D Open Structures: Slotted Rectangular Waveguide



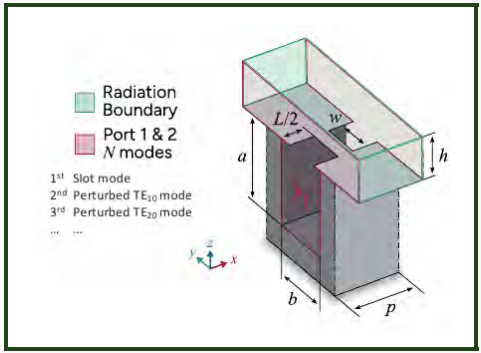


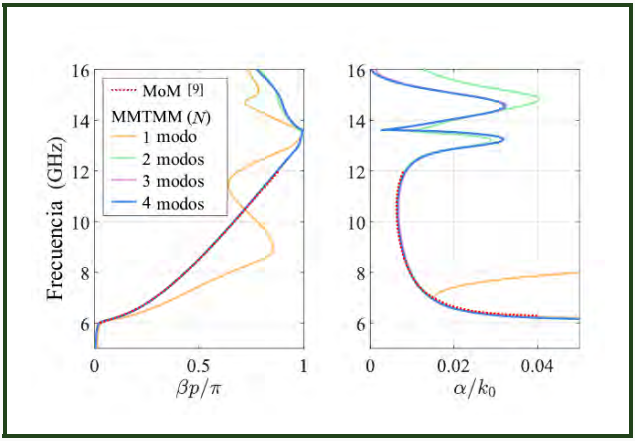
1-D Open Structures: Slotted Rectangular Waveguide



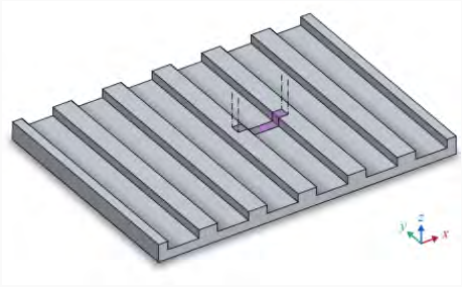


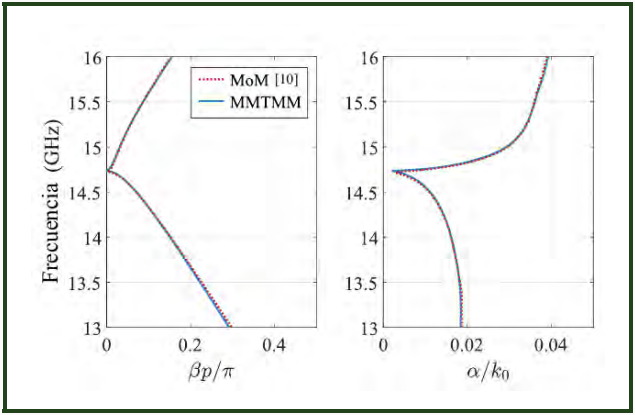
1-D Open Structures: Slotted Rectangular Waveguide



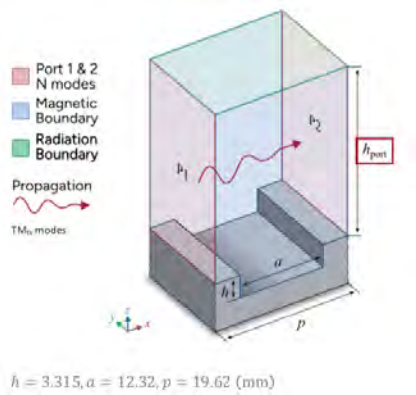


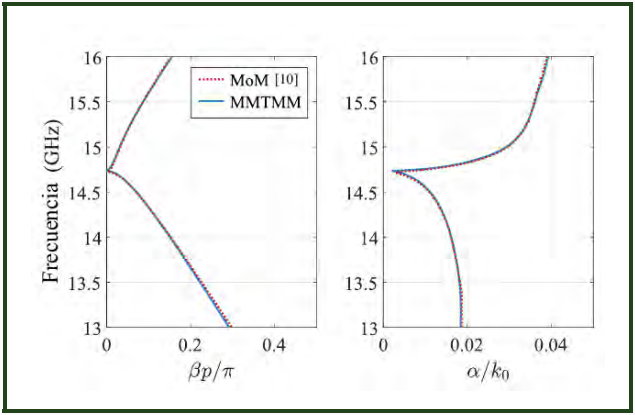
1-D Open Structures: Corrugated Waveguide



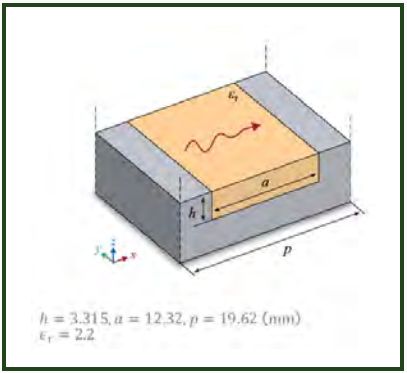


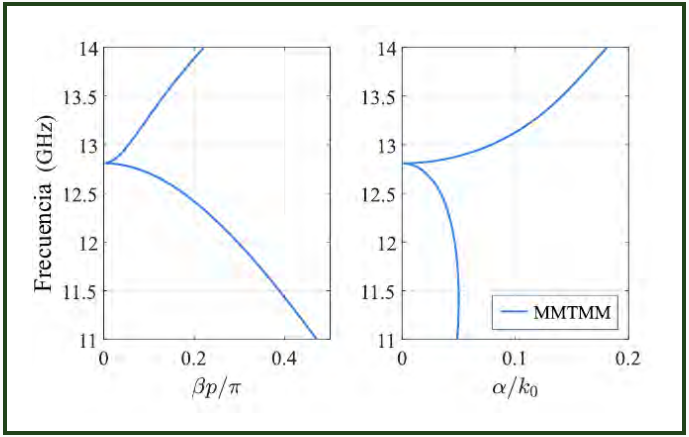
1-D Open Structures: Corrugated Waveguide



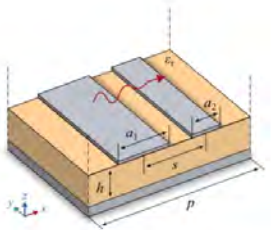


1-D Open Structures: Slotted Rectangular Waveguide with Dielectric

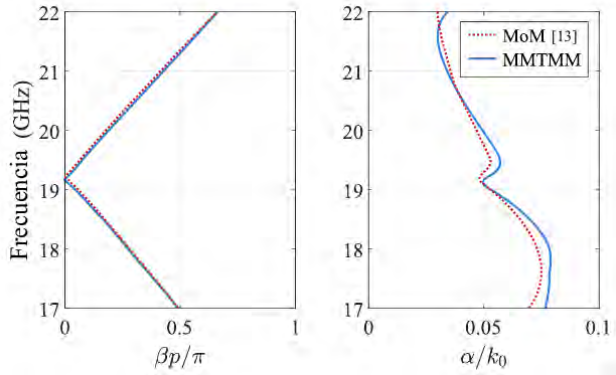




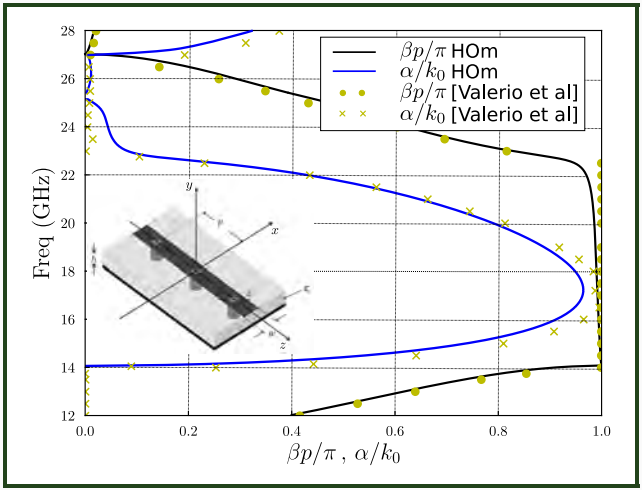
1-D Open Structures: Strip Gratings



$h = 1.27, a_1 = 1.2, a_2 = 0.96, s = 1.9, p = 8$ (mm)
$\epsilon_r = 10.2$

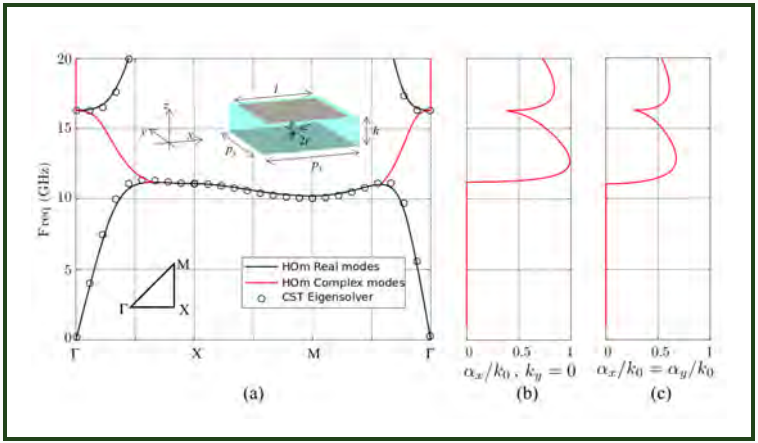


Microstrip leaky-wave antenna with vertical vias



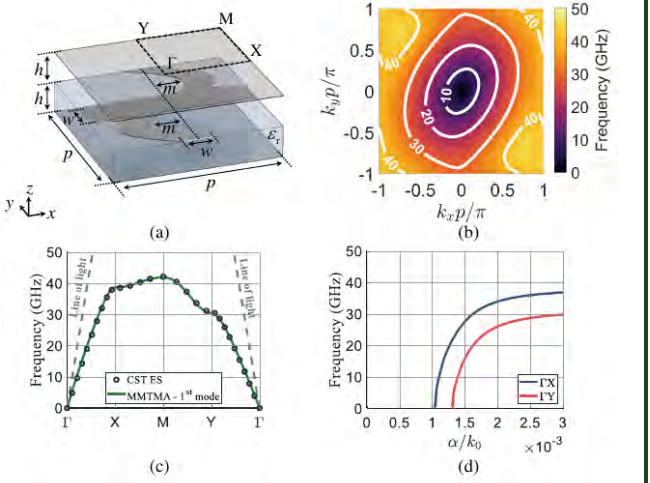
MMTMM results have been obtained with three modes ($M = 3$).

2-D periodic structure. Mushroom metasurface



$h = 1$ mm, $p_x = p_y = 3.5$ mm, $l = 3$ mm, $2r = 0.5$ mm, substrate with $\varepsilon_r = 2.2$.
(a) $\beta p/\pi$ in the irreducible Brillouin zone. α_x/k_0 with (b) $k_y = 0$ and (c) $k_y = k_x$.

2-D periodic structure. Anisotropic metasurface



Lossy substrate.

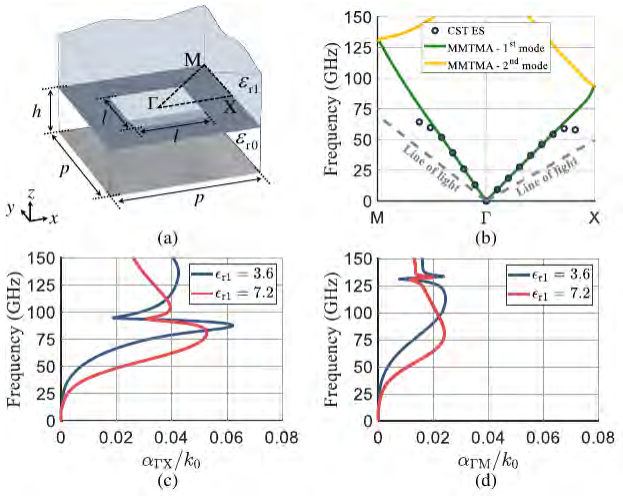
Isofrequency map very time-consuming by using commercial simulators.

Fig. 3. Bloch analysis of a 2-D metasurface consisting of printed meandered microstrip lines [24]: (a) Schematic of the unit cell. (b) Isofrequency map of the first mode, obtained computing only the upper half of the full Brillouin zone and rotating it by 180° around the center of the unit cell due to its 2-fold rotational symmetry. (c) Dispersion diagram of the first Bloch mode along the path $\overline{\Gamma X M Y \Gamma}$ depicted in pannel (a). (d) Normalized attenuation constant in the directions $\overline{\Gamma X}$ and $\overline{\Gamma Y}$. The dimensions are $p = 1.6$ mm, $w = 0.3$ mm, $m = 0.45$ mm, and $h = 0.3$ mm. The substrate is Rogers RO3035 with $\varepsilon_r = 3.6$ and $\tan\delta = 0.0015$ at 10 GHz.

Efficient Bloch Analysis of General Periodic Structures with a Linearized Multimodal Transfer-Matrix Approach

Federico Giusti, Qiao Chen, *Member, IEEE*, Francisco Mesa, *Fellow, IEEE*, Matteo Albani, *Fellow, IEEE*, and Oscar Quevedo-Teruel, *Senior Member, IEEE*

2-D periodic structure. Leaky-Wave metasurface



Efficient Bloch Analysis of General Periodic Structures with a Linearized Multimodal Transfer-Matrix Approach

Federico Giusti, Qiao Chen, *Member, IEEE*, Francisco Mesa, *Fellow, IEEE*, Matteo Albani, *Fellow, IEEE*, and Oscar Quevedo-Teruel, *Senior Member, IEEE*

Fig. 4. Bloch analysis of a 2-D squared hole unit cell which is open in the top: (a) Schematic of the unit cell. (b) Propagation constant in the directions ΓX and ΓM. (c) Normalized attenuation constant in ΓX ($\alpha_{\Gamma X}/k_0$) and (d) in ΓM ($\alpha_{\Gamma M}/k_0$). The dimensions as denoted in (a) are $p = 1.6$ mm, $l = 0.8$ mm and $h = 0.5$ mm; $\varepsilon_{r0} = 1$ and $\varepsilon_{r1} = 3.6$.

PEC required by CST Eigensolver on top of the metasurface. (🤨)

3-D periodic structure.

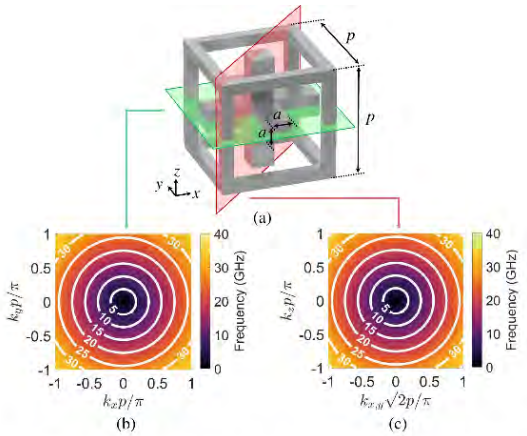


Fig. 5. Bloch analysis of 3D double-wire-mesh metamaterial: (a) Schematic of the unit cell. (b-c) Isofrequency plots of the two cuts illustrated in (a). The dimensions as denoted in (a) are $p = 4$ mm and $a = 0.8$ mm.

Efficient Bloch Analysis of General Periodic Structures with a Linearized Multimodal Transfer-Matrix Approach

Federico Giusti, Qiao Chen, *Member, IEEE*, Francisco Mesa, *Fellow, IEEE*, Matteo Albani, *Fellow, IEEE*, and Oscar Quevedo-Teruel, *Senior Member, IEEE*

Fig. 4. Bloch analysis of a 2-D squared hole unit cell which is open in the top: (a) Schematic of the unit cell. (b) Propagation constant in the directions $\overline{\Gamma X}$ and $\overline{\Gamma M}$. (c) Normalized attenuation constant in $\overline{\Gamma X}$ ($\alpha_{\Gamma X}/k_0$) and (d) in $\overline{\Gamma M}$ ($\alpha_{\Gamma M}/k_0$). The dimensions as denoted in (a) are $p = 1.6$ mm, $l = 0.8$ mm and $h = 0.5$ mm; $\varepsilon_{r0} = 1$ and $\varepsilon_{r1} = 3.6$.

Straightforward extension to 3-D structures.

Concluding remarks

Conclusions

- The most general and reliable method to compute the dispersion diagram of periodic structures is the numerical solution of Maxwell's equations in the unit cell of the structure subject to periodic boundary conditions. The major disadvantage of this rigorous eigenvalue approach is that it usually involves developing non-systematic in-house codes.
- The *N*-cell-cascade approach (Method A) is an alternative combined approach that allows for the use of commercial simulators. Valid when HOM interaction between unit cells is negligible.
  - A cascade of *N* unit cells is required to account for the inter-cell coupling due to high-order modes.
  - 2-port equivalent networks can only work in the monoband regime of the housing waveguiding system.
  - Method plagued with different numerical problems.
- Glide-symmetric structures would likely require the modeling of the unit cell as a multi-mode equivalent network, or the solution of the corresponding rigorous eigenvalue problem.
- The multi-mode transfer-matrix method (Method B [MMTMM]) is found to be a very convenient approach since it combines the advantages of commercial simulators at the cost of a little bit of in-house post-processing.

Thank you very much for your attention!

Adage:

> *Science never solves a problem without creating ten more.*
>
> George Bernard Shaw